DBAS-SLSTM: A Multi-Sensor Fusion Approach for Real-Time Motion Attitude Error Detection and Correction

Zhongyi Ni
Department of Police Physical Training and Tactics, Hubei University of Police, Wuhan, Hubei, 430034, China
Corresponding author's E-mail: nizy-zhongyi@outlook.com

Keywords: motion attitude, posture error detection, multi-sensor data, physical exercise training, joint angle analysis, dynamic beetle antennae search-driven stacked long short-term memory (DBAS-SLSTM)

Received: September 28, 2025

Efficient and accurate posture assessment is essential in physical exercise training to enhance performance, prevent injuries, and support overall well-being. This research aims to develop a Motion Attitude Error Detection System capable of continuously monitoring and correcting human movement using multi-sensor data. The proposed system integrates inertial measurement units, accelerometers, gyroscopes, and vision-based key-point tracking to capture comprehensive motion information. Experiments were conducted using the Motion Attitude Error Detection Dataset, consisting of 4,800 labeled motion sequences representing correct and incorrect postures. Raw sensor signals were preprocessed using a Kalman filter for noise reduction and Z-score normalization for scale consistency. Feature extraction using Wavelet Transform (WT) was then performed to compute joint angles, limb orientations, stability indices, and angular displacement metrics from fixed-length temporal windows. The proposed framework combining rule-based constraints with a Dynamic Beetle Antennae Search–optimized Stacked Long Short-Term Memory (DBAS-SLSTM) model was employed to learn spatiotemporal motion patterns, detect deviations from reference postures, classify error severity, and predict corrective movements. The system also provides real-time visual and auditory feedback to guide users during training. Experimental validation in a MATLAB environment, using a 70%-30% training–testing split, achieved an accuracy of 98.12%, along with high precision, recall, and F1-score values, demonstrating statistically reliable performance. The results confirm that the proposed approach offers a scalable, accurate, and practical solution for posture monitoring in sports training, rehabilitation, and ergonomic applications.

Povzetek: Raziskava razvija sistem, ki z uporabo senzorjev in računalniškega vida samodejno spremlja držo pri gibanju, zazna napake in v realnem času pomaga pri popravkih.

1 Introduction

The attitude of human motion that refers to the direction and the movement of the body in 3D space is one of the most important parameters in such areas as sports science and rehabilitation, as well as human-computer interaction [1]. Exact measurement of motion is critical in the objective evaluation of physical exercise performance, finding the wrong form and injury prevention. This field has been revolutionized by the introduction of miniaturized and inexpensive inertial measurement units (IMUs) that are usually multi-sensor systems of accelerometers, gyroscopes, and magnetometers [2]. These sensors are able to provide a rich stream of data that is able to estimate the kinematic parameters like joint angles, angular velocity, and linear acceleration. When it comes to physical exercise training, the technology allows the transition from the subjective, coach-based visual analysis to the objective, quantitative movement pattern analysis [3,4]. The main difficulty, though, is to strongly integrate such multi-sensor data to come up with a true and drift-free estimate of the actual attitude of the body, and based on which the error can be observed. Figure 1 shows diverse applications for monitoring, training, ergonomics, and safety.

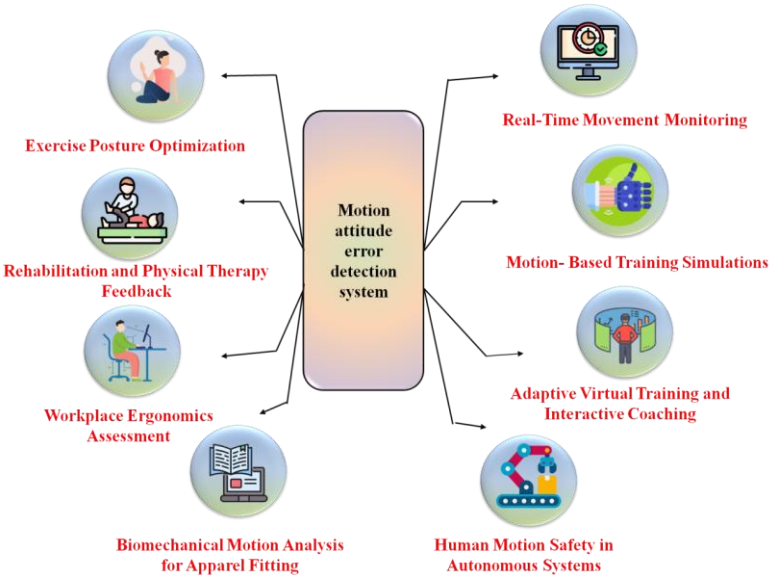

Figure 1: Applications of the motion attitude error detection system

The main idea behind this process is that the accurate recording of the kinematic information is revolutionized by the introduction of inertial measurement units (IMUs) [5, 6]. They are multi-dimensional and can be used to measure human movement in real-time, without being confined to laboratory conditions, as these sensors usually include accelerometers, gyroscopes, and magnetometers to give a rich stream of data [7]. The combination of this multisensor information is required to counteract the basic drift and noise of any single sensor to form a solid basis of motion tracking. It is an error detection which consists of the following physical exercise: inconsistency or deviation of anticipated sensor output and real sensor output [8]. With the assistance of filtering techniques and sensor fusion algorithms, the system can identify anomalies and eliminate noise as well as improve the overall accuracy of measurements [9]. It not only improves the functionality of the system but also provides stability in real-time. It can be extremely useful in a wide variety of contemporary technological uses by enhancing accuracy, safety, and efficiency through the use of multi-sensor data [10].

The accuracy and reliability of attitude and heading measurements in dynamic environments were improved using a Micro-Electro-Mechanical Systems (MEMS) multi-sensor fusion-based Attitude and Heading Reference System (AHRS) [11]. Results confirm improved error correction, numerical stability, and precise attitude positioning, demonstrating feasibility in practical engineering applications. The accuracy of a low-cost attitude observation sensor for the Wave Glider (WG)was examined by developing a multi-sensor hierarchical data fusion algorithm using an improved covariance matching adaptive Unscented Kalman Filter (UKF) [12]. Results demonstrate superior adaptability, stability, and precision in attitude estimation. The design of a multi-sensor data fusion (MSDF) system of motion trajectory monitoring among athletes was approached by [13]. The approach includes the combination of various sensors, system architecture design, and the use of high-level data fusion algorithms. Findings show enhanced accuracy, real-time updates of 20Hz, and flexibility with different sports. Possible limitations were the possible cost of the sensors, the complexity of the system, and the inability to reach extreme motion conditions.

The objective of attaining the proper 3-D human motion capture with the help of wearable inertial sensors in the absence of magnetic interference was suggested by [14]. The approach combines 9-axis sensor data through an extended Kalman filter, heuristic drift mitigation, and position estimation using the foot-mounted zero-velocity-update (ZUPT) method, and was summed up into a biomechanical model. The findings indicate enhanced motion tracking compared to the traditional methodologies. The drawbacks were the dependency on sensor location and the possibility of errors with dynamic movements. To improve human arm motion tracking with an Inertial Measurement Unit (IMU) against environmental changes was suggested by [15]. The algorithm utilizes an Elman Neural Network (ENN) to optimize refined Euler angles data that were pre-processed and calibrate the acceleration inputs without a magnetometer. Findings indicate a mean error of about 35mm and 37.2% x-axis betterment compared to standard procedures. The weaknesses were relying on standardized movements and might not perform well in high-dynamic or irregular movements. To develop a human motion capture system based on MEMS sensors and Zigbee wireless networks was approached by [16]. The process includes the implementation of several sensor nodes on the body, complementary filter data fusion, and processing data to calculate the trajectory and identify motions. Findings reveal an increase in efficiency by 10% and an increase in accuracy by 15%, whereas the limitations related to the location of the sensors and the possible

interference of the network. Table 1 summarizes the existing motion analysis approaches, highlighting the objectives, key outcomes, performance metrics, and inherent technical limitations.

Table 1: Related work of motion analysis and human activity in error detection

Reference	Method	Aim	Outcome	Limitations
Brunson et al. [17]	Generic Multisensor Integration Strategy (GMIS) + Variance Component Estimation (VCE) multi-IMU integration	Improve navigation and positioning accuracy	Positioning 14–16%, roll/pitch 30%, heading 40%	Requires multiple calibrated IMUs and complex integration
Zhong et al. [18]	Multilocal linearization with quaternion generation	Improve in-motion initial alignment	Higher accuracy and robustness than Optimization-Based Alignment (OBA)	Performance depends on measurement quality
Hajjej et al. [19]	IMU + quaternion filtering + LSTM	Human motion detection for healthcare e-learning	85.18% accuracy on wearable datasets	Sensitive to data quality and real-world motion variability
Dai et al. [20]	Multi-Scale Dependency (MSD) neural network for IMU anomaly detection	Detect IMU anomalies with interpretability	F1-score 95% with explainability	Computationally intensive
Li et al. [21]	Wireless smart glove with multi-IMU fusion	Hand motion tracking for rehabilitation	Accurate 3D tracking and joint repeatability	Limited to hand/finger motions
Gu et al. [22]	Magnetic-Inertial Measurement Units (MIMUs) real-time data fusion	Reduce magnetic disturbance errors	RMSE: knee 1.23°, hip 1.15°, elbow 3.67°	Susceptible to extreme magnetic noise
Liu et al. [23]	Unscented Kalman Filter (UKF)-based multi-sensor fusion for Unmanned Surface Vehicle (USV)	Enhance navigation under uncertainties	Improved accuracy and reliability	Application-specific to marine environments
Naseer et al. [24]	Random Forest Long Short-Term Memory (RFL)	Exercise pose estimation in therapy	High classification accuracy	Model complexity and sensor dependency
Chen and Fan, [25]	Convolutional Neural Networks (CNN) and CNN-Long Short-Term Memory (CNN-LSTM)	Exercise recognition and health prediction	mAP 78.6%, PCK@0.5 91.5%	Vision-based; sensitive to occlusion
Rao et al. [26]	Stereo vision + Bidirectional Convolutional Gated Recurrent Unit (Bi-CGRU)	Automated squat posture analysis	96.1% classification accuracy	Requires camera setup and lighting control
Charia et al. [27]	MediaPipe + Bidirectional Gated Recurrent Unit (Bi-GRU) with attention	Squat-type recognition and correction	94% accuracy	Limited generalization beyond squat actions

Traditional methods of detecting motion attitude errors are grounded in Machine Learning (ML) and Deep Learning (DL). Classifying and finding the patterns of errors with ML algorithms, such as the Support Vector Machine (SVM) and the random forest (RF), in comparison with auto-discovering features with DL algorithms, such as Convolutional Neural Networks (CNNs) and Recurrent Neural Networks (RNNs), are more suitable in more dynamic environments.

Motion attitude error detection limitations include high requirements in large labeled datasets, which are, in many cases, hard to acquire. ML models are not always good at nonlinear relationships, whereas DL methods consume large amounts of computational resources.

Moreover, the two approaches are vulnerable to processing problems in real-time, sense noise, and the ability to generalize well to different dynamic conditions.

1.1 Research questions

1. How effectively can the proposed DBAS-SLSTM framework detect deviations from reference human postures using multi-sensor IMU data in real time?
2. To what extent does DBAS–based parameter optimization improve classification accuracy and robustness compared to non-optimized SLSTM models?
3. How accurately can the proposed system classify posture error severity and predict corrective movements under varying sensor noise and user motion conditions?

The aim was to develop a robust motion attitude error detection system using multi-sensor data, integrating rule-based logic with a DBAS-SLSTM model to accurately detect deviations, classify error severity, and predict corrective movements for enhancing precision, reliability, and real-time performance in human motion monitoring. The following shows the key contribution of the research.

Data Collection: Collected various physical exercises, including squats, push-ups, lunges, and jumping jacks, covering diverse exercises, enabling accurate posture analysis and real-time motion monitoring.

Data Preprocessing: Applied a Kalman filter to remove sensor noise and Z-score normalization to standardize measurements, ensuring clean and consistent input signals.

Feature Extraction: Used Wavelet Transform to extract joint angles, limb orientations, and stability metrics, capturing both time-frequency motion characteristics effectively.

Proposed Method: Developed a DBAS-SLSTM hybrid framework combining rule-based logic and deep learning for real-time posture error detection and corrective feedback.

1.2 Research gaps

Multi-sensor fusion-based AHRS based on an extended Kalman Filter used by MEMS can still experience lower performance in very dynamic or vibration-intensive conditions, restricting the ability to work in extreme conditions [11]. Although the Wave Glider multi-sensor hierarchical data fusion technique is more accurate with low-cost sensors, it can be scaled down to large-scale or high-noise GPS signals [12]. Also, the USV navigation system based on UKF may be vulnerable to sudden environmental disruptions such as strong ocean currents, and this may interfere with the real-time accuracy [23].To address these issues, a two-tiered computational framework incorporating rule-based logic, in addition to a DBAS-SLSTM model, is used to identify posture deviations, categorize the extent of the error, and predict correctional movements, which improves accuracy, flexibility, and real-time operation under dynamic circumstances.

2 Methodology

Data collection involved acquiring multi-sensor motion data collected from participants performing various physical exercises from the Motion Posture Monitoring Dataset. Data preprocessing applied a Kalman filter to remove noise and Z-score normalization to standardize measurements. Feature extraction was performed using the Wavelet Transform to compute joint angles, limb orientations, and stability metrics. The proposed method employs a hybrid framework combining rule-based logic and a DBAS-SLSTM model for real-time motion error detection, severity classification, and corrective feedback. Figure 2 illustrates the overall flow of methodologies.

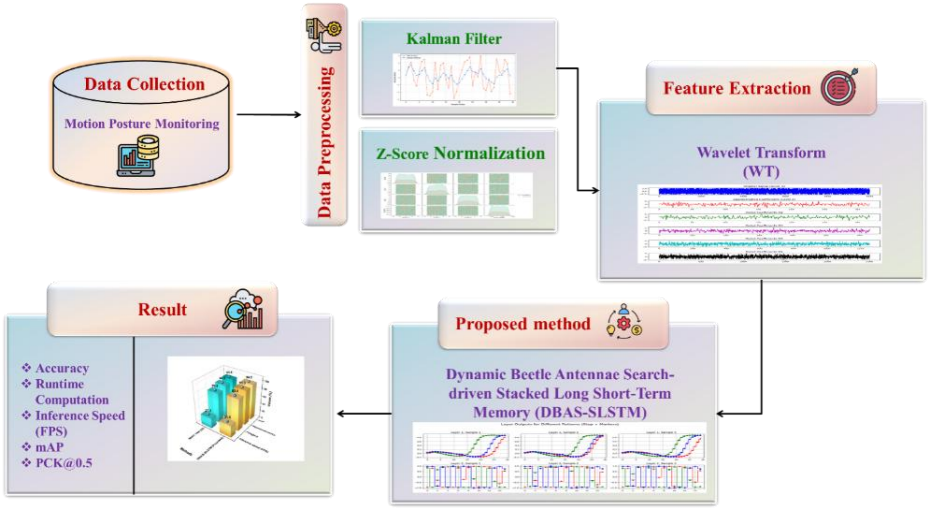

Figure 2: Overall flow in motion error detection in physical exercise

2.1 Data collection

The Motion Attitude Error Detection Dataset (https://www.kaggle.com/datasets/ziya07/motion-attitude-error-detection-dataset/data/data) is composed of 5,000 motion sequences, which are obtained at the time of physical exercise activities, and each motion sequence is a sequence of 3 seconds long, recorded with a fixed temporal window length. Each sample has flattened multi-sensor characteristics based on the measurements of inertia, such as joint angles and accelerator signals. The dataset is classified into two categories, namely, a correct posture (2,520 samples) and a posture error (2,480 samples), and it is balanced. The data were randomly split with 70% training and 30% testing data, and no overlapping subjects across each split. This open network facilitates reproducibility and valid comparison between posture error-detecting models.

2.2 Data preprocessing using kalman filter

The Kalman filter combines multi-sensor measurements, dampens noise, and predicts correct motion states to enhance the Motion Attitudes Error Detection System's functionality to track, assess, and correct human movements in real time effectively. State space, which is made up of state equations and observation equations, describes the Kalman filter. The following describes the equations that illustrate the system's dynamic properties in equation (1).

$$W_{l+1} = BW_l + B\mu_l + \omega_l$$
$$Y_l = GW_l + w_{l_1} \quad (1)$$

Where Y_l is the measuring vector, G is the observational matrix, u_l is a random noise vector,W_{l+1} is the next time step state vector, W_l denoted by the system's state, B denoted by the state transitions matrix, A is the matrix of control variables, μ_l is a controlling factor, and ω_l is the noise or disturbance in the process. Kalman filtering across the state of the most recent measurement and the present measurement yields the best estimate of the state. ω_l and ω_l have covariances of R_l and Q_l, respectively. Two steps make up the Kalman filter's operation: the prediction step and the correction step. The two steps in the computation procedure are as follows in equations (2) and (3).

$$\widehat{W}_{l+1|l} = \mathrm{B}\widehat{W}_{l|l} + A\mu_l$$
$$O_{l+1|l} = \mathrm{BO}_{l|l}B^S + R_l \quad (2)$$
$$O_{l+1|l+1} = (\mathrm{J} - L_{l+1}G)O_{l+1|l}$$
$$L_{l+1} = O_{l+1}|lG^S(GO_{l+1|l}G^S + Q_{l+1})^{-1}$$
$$\widehat{W}_{l+1|l+1} = \widehat{W}_{l+1|l} + L_{l+1}(Y_{l+1} - G\widehat{W}_{l+1|l}) \quad (3)$$

Where the predicted system state vector at time step$l$ is denoted by $\widehat{W}_{l+1|l}$, the estimated the system state vector at the time step $l+1$ by $\widehat{W}_{l|l}$, $A\mu_l$ represents control matrix, $G^S$the predicted system state vector at the time step l by $\widehat{W}_{l+1|l}$, the estimated uncertainty matrix of the current state is denoted by $O_{l|l}$,$R_l$is the process noise covariance matrix value, the predicted estimate covariant matrix for the next state by $O_{l+1|l}$, and the Kalman filter gain at time step $l+1$ by L_{l+1} , J is theIdentity matrix, $\widehat{W}_{l+1|l+1}$ – Updated state estimate after incorporating measurement Y_{l+1}, and$(Y_{l+1} - G\widehat{W}_{l+1|l})$ – The measurement residual is the discrepancy between the actual and expected measurements. Another way to characterize the covariance matrix is as follows in equations (4) and (5).

$$f_{l+1} = W_{l+1} - \widehat{W}_{l+1|l+1}$$
$$O_{l+1|l+1} = F(f_{l+1}f_l^S + 1) \quad (4)$$
$$= F((W_{l+1} - \widehat{W}_{l+1|l+1})$$
$$\times (W_{l+1} - \widehat{W}_{l+1|l+1})^S) \quad (5)$$

The estimation error vector f_{l+1} represents the difference between the actual and estimated state at time $l+1$. The posterior covariance $O_{l+1|l+1}$ quantifies uncertainty after correction, computed using the function F and the transpose operation for f_l^S outer product calculations. By minimizing the covariance matrix, an estimating process known as the Kalman filter determines the optimal estimate of the state. The Kalman filter obtains a posterior using measured values and prior knowledge, refreshes it with measurements, and uses the prior result as the current value. Figure 3 displays the smoothed versus raw acceleration signals for participant motion tracking accuracy.

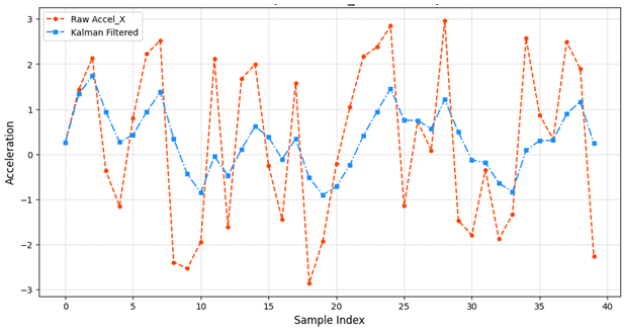

Figure 3: Kalman filtered for motion attitude error detection system

2.2.1 Z-score Normalization

Z-score normalization to standardize multi-sensor measurements, removing scale differences and reducing bias. This ensures consistent input for the motion attitude error detection system, enhancing accuracy in monitoring, evaluating, and correcting human movement in real time. Z-score normalization was a statistical standardization that ensured each feature was represented equally. It standardizes the data distributions to a mean of 0 and a standard deviation of 1, while still preserving relative relationships between features and structural transformations evenly. Equation (6) provides a numerical illustration of Z-score normalization.

$$Z = \frac{X-\mu}{\sigma} \quad (6)$$

Where μ represents the attribute mean, σ represents the feature standard deviation, Z represents the normalized value, and X represents the initial data value. The denominator $(X-\mu)$ in the equation above will position the data such that its mean is 0. It was subsequently scaled

to unit variance as 1 by multiplying $by\ \sigma$. Figure 4 shows the pairwise feature relationships colored by posture correctness after normalization.

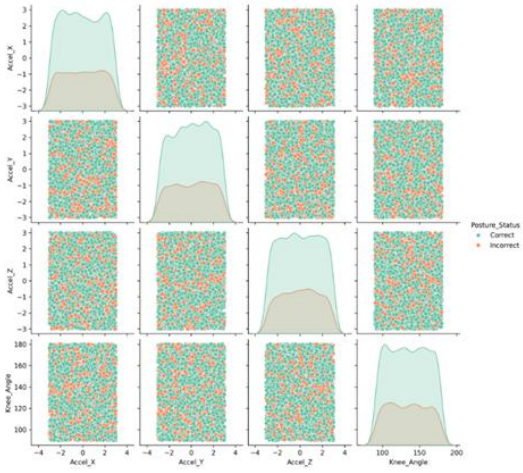

Figure 4: Normalized Multi-Sensor Distributions for Motion Attitude Error Detection System

2.3 Feature extraction using wavelet transform (WT)

Wavelet Transform (WT) enables the Motion Attitude Error Detection System to decompose multi-sensor signals into time–frequency components, capturing both transient and continuous movement patterns, enhancing accuracy in detecting, evaluating, and correcting human motion errors in real time. In comparison to traditional Fourier Transform (FT), which only offers global frequency content, or Short-Time Fourier Transform (STFT), which is limited to a particular fixed window, WT can behave simultaneously as a high-frequency transient and a low-frequency trend detector. Similarly, time-domain statistical characteristics that are simple might fail to detect fine dynamic changes in human movement. Therefore, WT is chosen to overcome these constraints yielding more detailed, multi-scale descriptions of motion signals to enhance the performance of the models. The continuous WT and the discrete WT are two types of wavelet transforms. The Continuous WT is translation invariant and permits wavelet transforms at all scales with continuous translation. In pattern-matching applications like discontinuity or chirp signal detection, the Continuous WT is frequently utilized. The Maximum detection section will provide further information about the CWT. The Discrete WT uses positions and scales that depend on a power of two. It is adequate for precise reconstruction, non-redundant, and more efficient. Consequently, the Discrete WT finds extensive application in feature extraction and data compression. Furthermore, vibration and wave propagation methods for damage assessment can be enhanced by incorporating wavelet transforms, enabling more accurate analysis of structural health.

A mass spectrum $t(p)$is broken down by the Discrete WT into an approximation component and multiple detailed components in equations (7) – (9).

$$t(p) = B_I(p) + \sum_{i<I} C_i(p), B_I(p) = \sum_{l\in Y} d_{I,l}\varphi_{I,l}(p) \quad (7)$$

$$C_i(p) = \sum_{l\in Y} c_{i,l}\psi_{i,l}(p), d_{i,l} = \langle t(p), \varphi_{i,l}(p)\rangle \quad (8)$$

$$c_{i,l} = \langle t(p), \psi_{i,l}(p)\rangle, i, l \in Y \quad (9)$$

Where B_I is the approximate element at the level$I$, C_i is the comprehensive component at level$i$, and I is the overall level of the DWT transform. The wavelet coefficient of B_I, orC_i, is the inner product of the scaling function $d_{I,l}$ at level I with translation l and the spectrum $t(p)$. Likewise, the wavelet coefficients of$c_{i,l}$,$\varphi_{I,l}$ is the inner product of the wavelet functional $\psi_{i,l}$at levels i with translations l and the spectrum$t(p)$. The WT$\psi_{i,l}$ and scaled function ($\psi_{i,l}$) expands by a factor of two as the level i increases;$l \in Y$ – Translation index; shifts the scaling function along the signal for analysis across time, $\sum_{l\in Y}$ the wavelet shifts to the right as l increases. Mallat's technique with filter banks requires P(M)operations to estimate the Discrete WT coefficient of a length M spectrum. The $c_{i,l}$ represents the detail component at the level i and translation l, extracted using the wavelet function $\psi_{i,l}(p)$, which captures high-frequency or transient features. Similarly, the inner product $\langle t(p), \varphi_{i,l}(p)\rangle$ computes the approximation coefficient $d_{i,l}$, while $\langle t(p), \psi_{i,l}(p)\rangle$ calculates the detail coefficient, quantifying signal features across scales and positions. Figure 5 shows that the multi-level signal decomposition reveals frequency components for movement analysis.

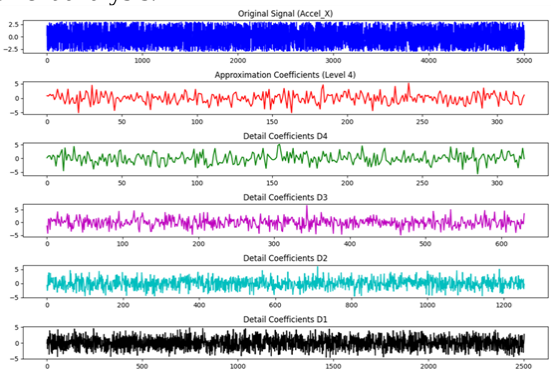

Figure 5: Wavelet-based feature extraction for motion attitude error detection system

2.4 DBAS-SLSTM to detect deviations from reference postures, classify error

severity, and predict correct movements

The DBAS-SLSTM model is proposed for a Motion Attitude Error Detection System utilizing multi-sensor data to monitor, evaluate, and correct human movements in real time. The system integrates accelerometers, gyroscopes, and magnetometers to capture comprehensive motion patterns. The Stacked LSTM element can learn temporal relationships and non-linearity of human motion and hence accurately capture anomalies of the right postures.

Adaptively control the proposed framework of DBAS-SLSTM, which bears high conceptual resemblances to other adaptive fuzzy control and neural adaptive control strategies applied in nonlinear and uncertain dynamic systems. The model, like adaptive controllers, continuously changes its internal parameters, responding to real-time sensor uncertainties and posture deviations, and allows for robust error detection and correction. The parameter tuning mechanism implemented based on DBAS is analogous to the adaptive gain adjustment mechanism, as it provides stability, rapid convergence, and resistance to sensor noise in a closed-loop feedback system. The DBAS algorithm is adaptively tuned to adjust network parameters and maximize convergence to achieve robustness in the conditions of noisy sensors. The model enables timely posture error detection, the degree of its severity, and corrective instructions. The experimental outcomes indicate a higher level of performance in terms of latency to reduce motion error detection and enhance accuracy in prediction, and thus, the system can be applied in sports training, rehabilitation, and ergonomic assessment, where continuous observation is crucial and quick feedback is essential. Pseudocode 1 shows the procedure of DBAS-SLSTM.

Pseudocode 1: DBAS-SLSTM

Inputs:
- *Multi − sensor data streams*:
  Accelerometer $A[t]$, *Gyroscope* $G[t]$, *Magnetometer* $M[t]$
- *Hyperparameters*:
  Sequence length $= 50$ *timesteps*
  Learning rate $= 0.001$
  Number of SLSTM layers $= 2$
  Hidden units per layer $= 64, 32$
  Dropout rate $= 0.4$
  Activation functions: *ReLU* (*Dense*), *Softmax* (*Output*)
  DBAS step size $\delta = 0.5$
  Decay factor $\alpha = 0.9$
  Number of exploration directions $P = 4$
  Total iterations $S = 100$
  Optimizer $=$ *Adam*

Outputs:
- *Detected posture errors*
- *Severity score* $(0 - 1)$
- *Corrective instructions*

Step 1: *Preprocessing*
1.1 *Normalize sensor inputs* $A[t], G[t], M[t]$ *to range* $[-1,1]$.
1.2 *Construct input sequence* $J[t]$ $= [A[t], G[t], M[t]]$ *of length* 50.
1.3 *Apply wavelet decomposition to remove high* $-$ *frequency noise.*

Step 2: *Forward Pass through SLSTM*

For each timestep s in sequence $(1 \ldots 50)$:
Forget Gate
$e\_s = \sigma(X\_e * [g\_(s-1), w\_s] + a\_e)$
Example: $e\_ = \sigma(0.8 * [0.3, 0.5] + 0.2)\ 0.62$
Input Gate
$j\_s = \sigma(X\_j * [g\_(s-1), w\_s] + a\_j)$
Example: $j_s = \sigma(0.5 * [0.3, 0.5] + 0.1) 0.58$
Candidate Cell State
$\tilde{D}\_s = tanh(X\_D * [g\_(s-1), w\_s] + a\_d)$
Example: $\tilde{D}_s\ tanh(0.7 * [0.3, 0.5] + 0.1)\ 0.45$
Cell State Update
$D\_s = e\_s * D\_(s-1) + j\_s * \tilde{D}\_s$
Example: $D_s = 0.62 * 0.4 + 0.58 * 0.45 \approx 0.49$
Output Gate
$p\_s = \sigma(X\_p * [g\_(s-1), w\_s] + a\_p)$
Example: $p_s = \sigma(0.6 * [0.3, 0.5] + 0.2) \approx 0.66$
Hidden State
$g\_s = p\_s * tanh(D\_s)$
Example: $g\_s = 0.66 * tanh(0.49) \approx 0.31$

Step 2.5: *Training Loop*
- *Number of epochs* $= 50$
- *Batch size* $= 32$ **
- *Loss function* $=$ *Categorical Cross − Entropy* $+$ *MSE for severity*
- *Track training/validation loss and accuracy*
- *Generate learning curves for convergence visualization*

Return sequence of hidden states g_s*to Dense Layers.*

Step 3: *Dense Layers for Posture Error Prediction*
3.1 *Fully Connected Layer* (*ReLU*, 128 *units*).
3.2 *Dropout Layer* ($rate = 0.4$).
3.3 *Fully Connected Layer* (*Softmax*, 2 *units*: *Correct vs Error*).
3.4 *Output*:
- $y\_pred \in \{0,1\}$ (*posture classification*)
- *Error severity score* $\in [0,1]$.

Step 4: *Dynamic Beetle Antennae Search* (*DBAS*) *Optimization*
Initialize:
$\delta = 0.5, \alpha = 0.9, iteration\ s = 1$
$W\_best = random\ weight\ initialization$
While $s \leq S$ (100 *iterations*):
 # Step Update
$\delta\_(n+1) = \delta * \alpha\text{^}s$
Example: $\delta\_(2) = 0.5 * 0.9\text{^}2 = 0.405$
Multi − Directional Exploration
Generate $P = 4$ *random exploration vectors* $\vec{c}$
$w\_left = W\_best + \delta\_(n+1) * \vec{c}$
$w\_right = W\_best - \delta\_(n+1) * \vec{c}$
Evaluate Fitness (*Loss Function*)
$f\_left = Loss(SLSTM(w\_left))$
$f\_right = Loss(SLSTM(w\_right))$
Update Best
If $f\_left < f\_right$:
$W\_best = w\_left$
Else:
$W\_best = w\_right$
Lens Opposition − Based Learning (*LOBL*)
$midpoint = (a\_i + b\_i)/2$
$W'\_best = midpoint + (midpoint/-W\_best/m)$
If $Loss(W'\_best) < Loss(W\_best)$:
$W\_best = W'\_best$
Increment iteration $s = s + 1$
Return optimized parameters W_best.

Step 5: *Posture Correction Feedback*
If y_pred == "*Error*":
Display corrective instruction (*e.g.*, "*Straighten your back*")
Show severity score (*e.g.*, $0.73 =$ *moderately severe*)

End Algorithm with Model Summary Table
- *Include a table listing each layer, units, activation, dropout, and output*

– Include learning curves showing training /validation loss and accuracy over epochs
End Algorithm

Figure 6 shows how the multi-sensor data can be sequentially processed to detect posture deviation, classify the severity of posture deviation, and provide corrective feedback in real-time.

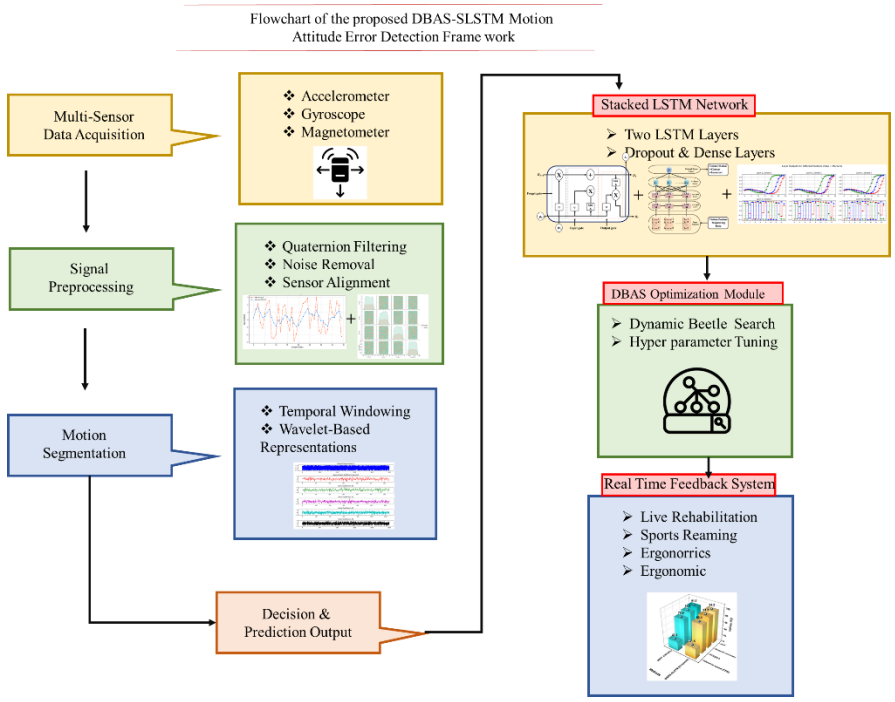

Figure 6: Architecture of the DBAS-SLSTM-based motion attitude error detection framework

2.4.1 Long short-term memory to identify the sequence that deviates from the correct pattern

LSTM networks are employed in the Motion Attitude Error Detection System to capture temporal dependencies in multi-sensor data, enabling accurate real-time monitoring, evaluation, and correction of human movements. By retaining relevant motion history, LSTM enhances posture recognition, detects deviations, and predicts corrective actions efficiently. Memory cells are the fundamental units of LSTM design. Despite being merely neurons in neural networks, these cells may learn and ignore irrelevant portions of past states, store pertinent new information in the cell, modify cell states selectively, and ultimately regulate the information transmitted. Through a sequence of LSTM units and temporal delays, the LSTM architecture's physical sense for runoff modeling enables it to preserve the sequential character of flow dependence to various rainfall stations. It allows it to forget in each memory cell structure and logs the relationship between various rainfall stations and runoff. Recently, a variety of LSTM-based models have been used for forecasting and runoff modeling. The following are the LSTM memory cell transition equations. Figure 7 shows the architecture of an LSTM.

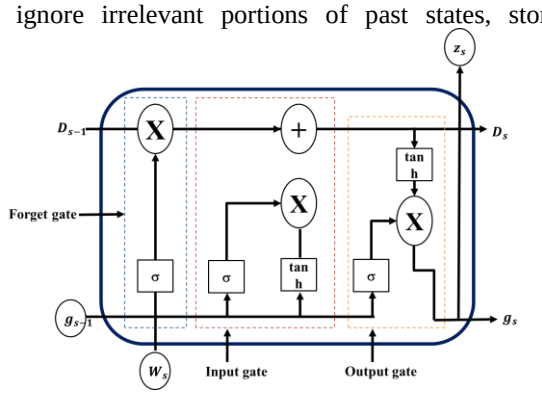

Figure 7: LSTM cell architecture for motion attitude error detection system

The first gate, referred to as the forget gate, determines which element of D_{s-1} must be forgotten by multiplying it by e_s, which ranges from 0 to 1. This is how the LSTM memory cell processes different information. Furthermore, w_s represents the cell's current input, g_{s-1} is the state of the preceding cell in the layer,σ denotes the sigmoid activation function, and X_e and a_e are trainable parameters in the forget gate in equation (10).

$$e_s = \sigma(X_e \cdot [g_{s-1}, w_s] + a_e) \quad (10)$$

The input gate, which comes next, is where the value that has to be updated is determined in equation (11).

$$j_s = \sigma(X_j \cdot [g_{s-1}, w_s] + a_j) \quad (11)$$

Where j_s value of the output variable ranges from 0 to 1. The input gate has two trainable parameters: X_j and a_j. Next, using the following equation, the possible vectors werethe current input (w_s), $tanh$ is the hyperbolic tangent function, and the final hidden state, g_{s-1}, in equation (12).

$$\widetilde{D}_s = \tanh\left(X_D \cdot \left[g_{s-1,w_s}\right] + a_d\right) \quad (12)$$

X_D and a_d are input gate parameters that may be taught throughout the training process, while $\widetilde{D}_s$ is a vector having values between 0 and 1.

The following formula is then used to determine D_s in equation (13).

$$D_s = e_s * D_{s-1} + j_s \times \widetilde{D}_s \quad (13)$$

In the output gate, the output is finally computed by using a sigmoid activation function in equation (14).

$$p_s = \sigma\left(X_p\left[g_{s-1,w_s}\right] + a_p\right) \quad (14)$$

Where the values of the vector p_s range from 0 to 1. $D_s = e_s * D_{s-1} + j_s \times \widetilde{D}_s$ updates the cell state by combining forgotten past and new input. $p_s = \sigma\left(X_p\left[g_{s-1,w_s}\right] + a_p\right)$ computes the output gate, and $g_s = p_s \times \tanh(D_s)$ determines the hidden state for the next time step. a_p and X_p are parameters that can be trained, p_s– Output gate controlling which parts of the cell state are exposed. g_s – Hidden state, the final output for the time step. The output is multiplied element-wise by the hyperbolic tangential angle of D_s to determine the new hidden state, g_s, as follows in equation (15).

$$g_s = p_s \times \tanh(D_s) \quad (15)$$

Stacked Long Short-Term Memory multiple layers to understand complex movement patterns

The SLSTM architecture is employed in the Motion Attitude Error Detection System to process sequential multi-sensor data. By capturing temporal dependencies and complex motion patterns, it enables real-time monitoring, evaluation, and correction of human movements, improving posture accuracy, preventing injuries, and enhancing overall exercise performance. Two LSTM layers combined with two completely connected dense layers for identifying the sequential structure of the problem, and a layer for dropout with a dropout rate of 0.4 on the initial fully connected layer for preventing overfitting, make up the suggested deep neural network architecture. Additionally, the C_1 *and* C_2 normalization method was used to lower the probability of the model overfitting byD_m maintaining small weight and bias values. To capture the effect of autocorrelation, input variables are converted to sequences due to the autocorrelated nature of stream flow.J_{s-m} represents a sequential input of multi-sensor measurements over time, J_s capturing past motion states for SLSTM processing. The last dense layer was the same for all basins, with one neuron signifying runoff output. The wavelet was utilized in both basins to identify independent variables, and the influence of convergence between variables in outflow modeling was also examined using basic normalized datasets. Figure 8 shows the suggested sequential machine learning in conjunction with a dense layer that is fully linked.

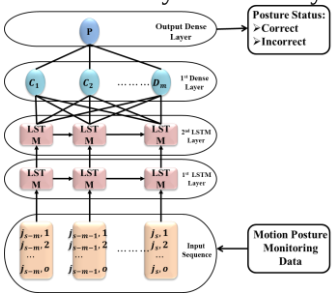

Figure 8: SLSTM architecture for sequential motion attitude error detection modeling

The algorithm's input sequence window is sequential information with m features and a o-day latency. Figure 9 shows the Layer-wise neural activations across samples for multi-sensor motion inputs.

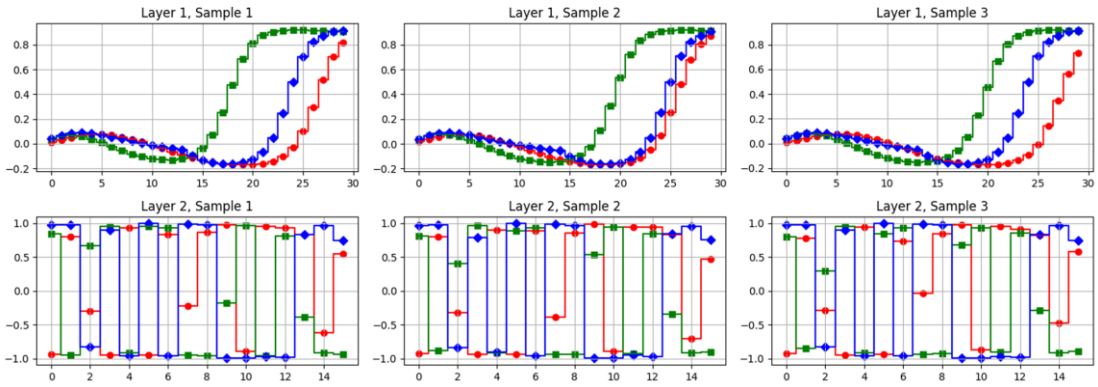

Figure 9: SLSTM layer outputs for real-time motion attitude error detection

2.4.2 Dynamic beetle antennae search selects the best possible architecture and settings for the SLSTM model

A DBAS algorithm is employed in the Motion Attitude Error Detection System to optimize multi-sensor data analysis, enabling real-time monitoring, evaluation, and correction of human movements. It efficiently searches for optimal parameters, enhances posture classification accuracy, and improves detection of subtle motion deviations. DBAS was selected as opposed to other popular optimization technologies like Bayesian Optimization and Genetic Algorithms (GA) due to the fact that it provides a single-search technique that is less expensive to compute, less complicated to parameterize, and converges more rapidly. The initial experiments show that DBAS has similar or even improved optimization performance in real-time posture error detection and requires fewer iterations. Its ability to be tuned to multi-dimensional optimization, as well as to respond to the dynamic variation of sensors, makes it especially favorable to the parameter tuning of SLSTM. Comparing the Beetle Antennae Search algorithm to other clever algorithms, it has the benefits of being a single search method with a low computational cost, low spatial complexities, and fewer necessary parameters. Its practical applicability is limited, nevertheless, by the ease with which it might slip into local optimum solutions when working with high-dimensional issues. The Beetle Antennae Search algorithm's narrow exploration direction and step's quick decline are the main factors.

The Adaptive Step Method: According to the BAS algorithm's concept, the performance of the BAS method is mostly based on the Beetle Antennae's step factor. The global search capacity will be more important, but the rate of convergence velocity would be slower if the searching step of the Antennae whisker decays slowly enough. The technique may converge before discovering the globally most effective approach because the search time decays too quickly. Therefore, to guarantee useful exploration and avoid premature convergence, a compromise between speed and the worldwide search capability of convergence is required in equation (16).

$$\begin{cases} \delta_{n+1} = \delta * \alpha^k \\ w_{left} = w_n + \delta_{n+1}\vec{c} \\ w_{right} = w_n - \delta_{n+1}\vec{c} \end{cases} \quad (16)$$

The beetle's left and right antennae locations during exploration are represented by the variables w_{left} and w_{right} , respectively. As the number of repetitions increases, the variable length of each step steadily decreases, and the difficulty of the desired issue may be taken into consideration while choosing α^k.In this case, $\delta$is the initial step length established, $\delta_{n+1}$is the initial step length $n+1th$ antenna exploration, w_n is the current position, $\delta_{n+1}\vec{c}$is the exploration step, and α is the step updating factor. For low-dimensional issues, the technique converges quickly; for high-dimensional issues with a wide exploration range, it converges slowly. The first BAS algorithm step determines the value of $\delta_{threshold}$, which is typically between 0.6 and 0.8 times. The method stays out of the rapid convergence phase as a result.

Multidirectional Approach to Exploration: The BAS method only randomly examines two symmetric directions; its exploration capabilities are restricted. The investigation of the method has various flaws, and it raises the possibility of overlooking the best answer close to the specified point. The algorithm's worldwide search capability is enhanced by the multi-directional search strategy from the outset. This technique increases the detection range by allowing the antennas to simultaneously investigate several directions. The formula for multi-directional exploration is as follows in equation (17).

$$\vec{c} = \frac{rand(m,P)}{||rand(m,P)||} \quad (17)$$

where $\vec{c}$ signifies the production of P pairs of exploration directions and $rand(m,P)$ denotes the random generation of P pairs of m-dimensional vectors. Whiskers on antennae must go in two distinct directions. Becomes too low, $rand$ inhibits the algorithm's development. P can have a range of numbers from $4\ to\ 6$, and depending on the situation, the specific value can be investigated.

Each beetle's location in equation (18) can be updated further using the following formula.

$$\begin{cases} w_{left} = w_n + \delta_{n+1}\vec{c_s}' \\ w_{right} = w_n - \delta_{n+1}\vec{c_s} \end{cases} (j \in [0,1]), \quad (18)$$

The beetle's left and right antennae locations during exploration are indicated by the variables w_{left} and w_{right}, respectively. w_n is the beetle's current position, and δ_{n+1} is the step length for the next iteration, determining how far the antennas probe in each direction. The notation $(j \in [0,1])$ indicates the selection of a specific antenna direction or weight for updating the beetle's position. This mechanism allows DBAS to balance exploration and exploitation efficiently. If $\vec{c_s}$ is used to update the position equation and $\vec{c_j}$ indicates the ith rows of $\vec{c}_s'$.

Learning Strategy Based on Lens Opposition: Lens Opposition-Based Learning (LOBL) combines inverse learning techniques with optical lens inverted physics to dynamically redirect optimization value from local extrema. In particular, LOBL uses a computational inversion "lens" to assess the "inverse image" solution when it converges onto poor solutions. In particular, LOBL uses a computational inversion "lens" to assess the "inverse image" solution when it converges onto poor solutions. Comparing incremental enhancements from current versus inverted vectors reveals better solutions. The technique increases the algorithm's ability to optimize globally, inhibits local optimization, and increases the number of feasible solutions. It is

effectively integrated with other algorithms to greatly increase the optimization capacity of the algorithm.

Equation19 defines a normalized position $\frac{g}{g'}$ for an agent within a bounded search space $\frac{b_i+a_i}{2}$. It relates the agent's current midpoint position to the best-known position $W_{best}(s)$ and a derived best position $W'_{best}(s)$, guiding iterative optimization, which corresponds to the global ideal outcome achieved via lens reflection.

$$\frac{\frac{b_i+a_i}{2}-W_{best}(s)}{W'_{best}(s)-\frac{b_i+a_i}{2}}=\frac{g}{g'} \quad (19)$$

After setting $\frac{g}{g'}=m$, $\frac{b_i+a_i}{2}$ is the midpoint of the search range, the equation W'_{best} is produced by the following transformation in equation (20).

$$W'_{best}(s)=\frac{(b_i+a_i)}{2}+\frac{(b_i+a_i)}{2m}-\frac{W_{best}(s)}{m} \quad (20)$$

It is possible to reduce the LOBL formula to the OBL formula when m equals 1. General inverse learning yields a fixed inverse solution. It alters the value of m,$W'_{best}(s)$ represents the opposite, enhancing global exploration. b_i and a_i are the lower and upper bounds of the exploration space in the $i-th$ dimension, with $\frac{(b_i+a_i)}{2}$ as the midpoint, serving as the lens center. $W_{best}(s)$ is the current global best position in the s-th dimension. The scaling factor m controls the range of inverse solutions, while $\frac{(b_i+a_i)}{2m}-\frac{W_{best}(s)}{m}$ represents the adjusted distance from the midpoint to the global best, scaled for exploration, enhancing the algorithm's capacity for global optimization. The optimization algorithm usually does a sensitive local search after a large-scale search; the interaction change in m in equation (21).

$$m=(1+(s/S)^{\frac{1}{2}})^{10} \quad (21)$$

As the number of iterations increases, the range of its inverted solution decreases, and the value of m grows; s is the current iteration and S represents the total number of iterations. Rising to the tenth power dynamically adapts, the square root grows smoothly, and the fraction s/S scales. Table 2 shows the hyperparameters of DBAS-SLSTM.

Table 2: Hyperparameters of DBAS-SLSTM

Component	Parameter	Value
DBAS Optimization	Number of beetles (N)	5
	Antennae distance (d)	0.1
	Step size (α)	0.05
	Max iterations (MaxIter)	10
Stacked LSTM	Number of layers (L)	2
	Hidden units per layer (H)	50
LSTM Training	Learning rate (η)	0.001
	Epochs	20
	Batch size	32
Training Protocol	Learning rate (η)	0.001
	Batch size	32
	Epochs	20

3 Results

The experiment setup was performed using MATLAB to implement the suggested method. To test the performance of inferences, the system was run on a PC with an Intel Core i7-9700 CPU, 16 GB RAM, and a NVIDIA GTX 1660 graphics card. The latency measurements show that the system provides feedback within 120150 ms per motion frame, which shows that it is close to real-time in this environment. The experimental results are explained in detail in this section. The following metrics were used to evaluate the suggested approach and ascertain its efficacy: Accuracy, Runtime Computation, Inference speed (FPS), mAP, and PCK@0.5. Additionally, a comparative analysis was carried out with other current methods, such as Bidirectional Recurrent Neural Network (Bi-RNN) [26], Bidirectional Long Short-Term Memory (Bi-LSTM) [26], Recurrent Neural Network with Attention Mechanism (RNN + Attention) [26], Bidirectional RNN with Attention Mechanism (Bi-RNN + Attention) [26], Bidirectional LSTM with Attention Mechanism (Bi-LSTM + Attention) [26], Bidirectional Convolutional LSTM (Bi-CLSTM) [26], Bidirectional Convolutional GRU with Attention Mechanism (Bi-CGRU + Attention) [26], Bidirectional Gated Recurrent Unit (Bi-GRU) [27], Bidirectional GRU with Attention Mechanism (Bi-GRU + Attention) [27], multi-scale feature fusion convolutional neural networks (MSFF-CNN) for posture recognition [25], Random Forest (RF) [24], Decision Tree (DT) [24], Logistic Regression (LR) [24], and Gaussian Naive Bayes (GNB) [24].

The Motion Attitude Error Detection System is an internal multi-sensor-based data detection system that operates on the internal data, which is the acceleration and angle of the joints, to monitor the movements of a human being in real time. Based on the DBAS-SLSTM model, it identifies posture and motion errors by comparing real movements and ideal patterns and gives corrective feedback. The system can be applied to sports, rehabilitation, and ergonomics. Figure 10 demonstrates patterns of movements in terms of the knee angles.

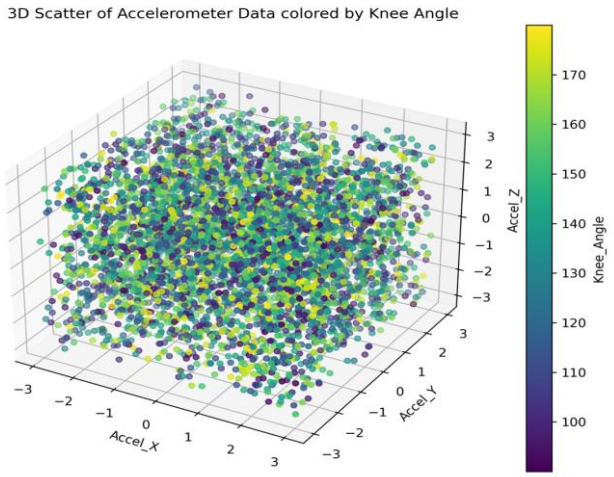

Figure 10: 3D Accelerometer scatter colored by real-time knee angle

The proposed system of detecting a motion attitude error incorporates multiple sensors, such as accelerometer measurements and joint angles, which allow the system to monitor human movement constantly. The DBAS-SLSTM model recognizes motion abnormalities in real time and allows immediate corrective feedback. This helps in improving posture, performance, and preventing injuries during sports, rehabilitation, and ergonomics. Figure 11(a) and 11(b) are Andrews and parallel plots that represent posture correctness.

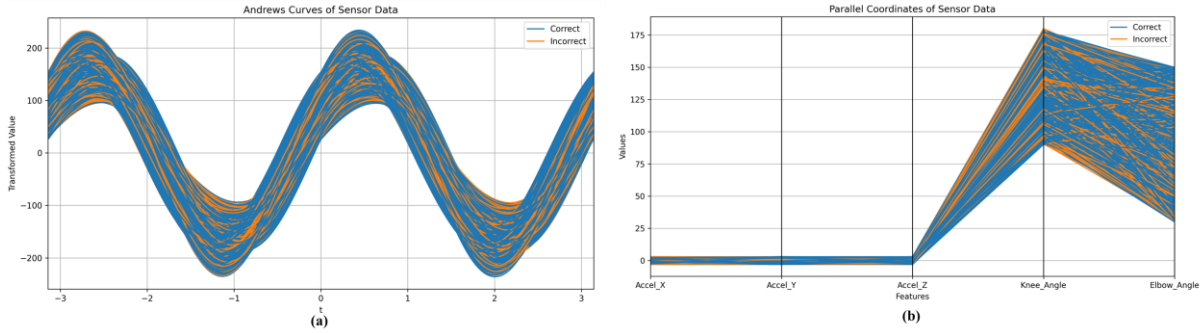

Figure 11: Visualization of (a) Andrews Curves, (b) parallel coordinates of sensor data in motion error detection

The motion attitude error detection system. The Motion attitude error system of detection is the system that utilizes real-time multisensor data, which comprises the joint angles and the acceleration, to analyze human movement. DBAS- SLSTM model is a model that examines stability and angular displacement to identify performance variations and give feedback. This promotes physical therapy, sports training, and ergonomics. Figure 12(a) represents a bubble diagram of joint stability, and Figure 12(b) represents a contour diagram of knee angle through acceleration.

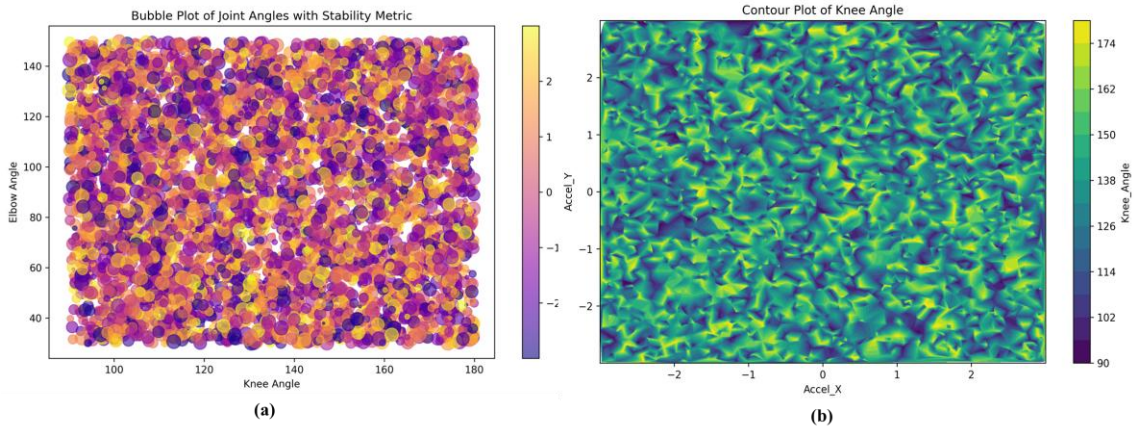

Figure 12: Analysis of (a) Bubble plot of joint angles, (b) Knee angle contour in motion detection

The proposed system combines the data of multiple sensors, such as joint angles and accelerometer signals, and implements the DBAS-SLSTM model to evaluate the human movement continuously. Deviation of anticipated paths imposes absent-mindedness in response and reconstruction. This method enhances rehabilitation, sporting training, and ergonomic assessment. Figure 13(a) represents the changes in the knee angle of the rolling means, whereas Figure 13(b) illustrates the time-dependent plot of the acceleration multi-axis stacked.

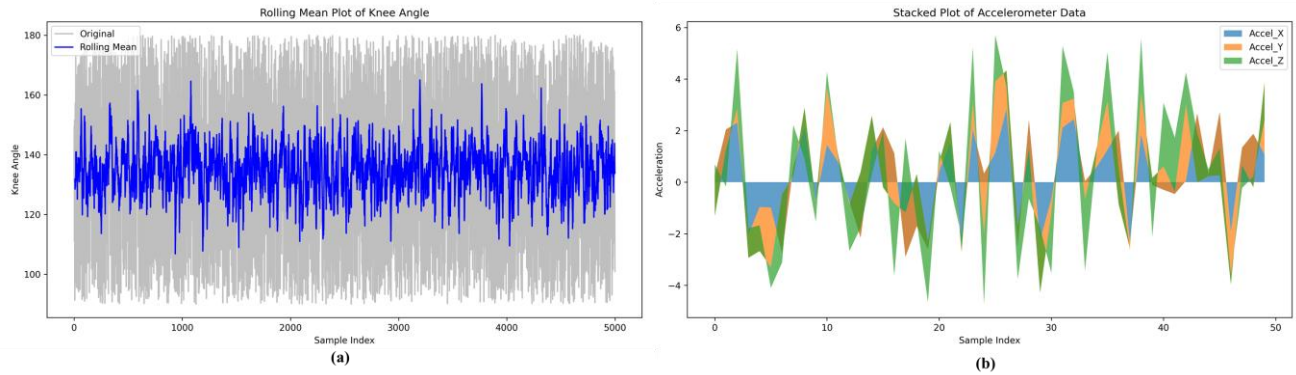

Figure 13: Depiction of (a) Rolling mean smoothing of knee angle data and (b) Stacked accelerometer signals across three spatial axes

The training and validation accuracy of the DBAS-SLSTM model in motion attitude error. Figure 14(a) indicates that the training loss decreases and the validation loss remains constant during the 200 epochs, which is a sign of successful learning. Figure 14(b) indicates that the accuracy of training and validation is high, indicating that the model can reliably and in real time capture human motion patterns.

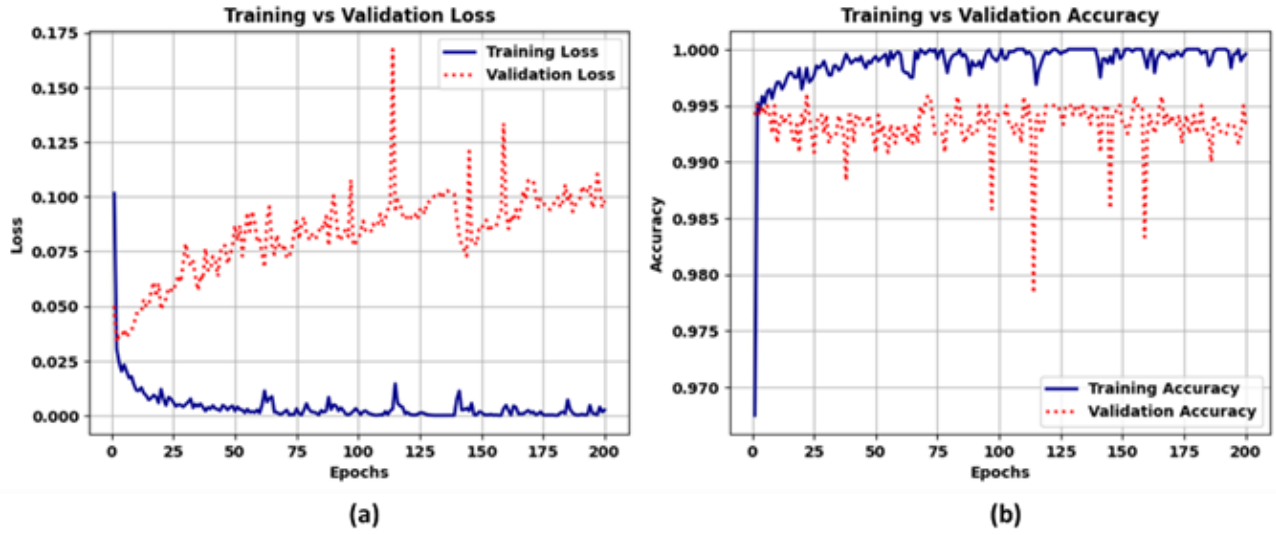

Figure 14: Training and validation (a) Loss and (b) Accuracy performance of DBAS-SLSTM for real-time motion attitude error detection

The computation of the performance of the proposed DBAS-SLSTM model was calculated by 5-fold cross-validation. The findings are presented in the form of mean values and 95% confidence intervals, and these figures illustrate the consistency and reliability of the model. The p-values are used to confirm that the obtained accuracy, the average Precision, and the actual speed of inference at that time are consistent and are not a result of random error, as reported in Table 3.

Table 3: Statistical validation of DBAS-SLSTM performance using 5-Fold cross-validation

Metric	Mean Value	95% Confidence Interval (CI)	p-value	Significance
Accuracy (%)	98.12	± 0.84	< 0.01	Significant
mAP (%)	83.40	± 1.27	< 0.05	Significant
Inference Speed (FPS)	31.5	± 0.6	< 0.05	Significant

The ablation research of the given system demonstrates the progressive effect of each component on the performance. Simple preprocessing, Kalman Filter, and Z-Score Normalization increase accuracy slightly, whereas WT increases feature representation. SLSTM is used to learn temporal dependencies, and DBAS to optimize model parameters. It has been shown that the proposed DBAS-SLSTM system can be the most accurate, with the highest mAP, and with the competitive speed of inference in real-time due to the presented effectiveness of the combined methodology, as shown in Table 4.

Table 4: Ablation research of DBAS-SLSTM on motion attitude error detection performance

Method / Component	Accuracy (%)	mAP (%)	Inference Speed (FPS)
Kalman Filter	84.12	68.45	35.2
Z-Score Normalization	86.57	70.91	34.8
Wavelet Transform (WT)	90.23	76.34	33.5
SLSTM	94.78	80.12	32.1
DBAS	96.85	82.74	31.7
DBAS-SLSTM [Proposed]	98.12	83.40	31.5

The runtime computation results indicate varying efficiency among the evaluated techniques. RF achieved 6.879s, DT 3.063s, LR 17.32s, and GNB 0.347s. Among traditional methods, GNB demonstrated the fastest performance. However, the proposed DBAS-SLSTM model outperformed all, recording the lowest runtime of 0.273s, highlighting its superior computational efficiency. This demonstrates that DBAS-SLSTM not only surpasses conventional machine learning methods but also offers a highly optimized solution for real-time motion attitude error detection. Table 5 shows execution times of methods, highlighting the fastest approach.

Table 5: Runtime comparison of techniques for motion error detection

Methods	Runtime Computation (s)
RF [24]	6.879
DT [24]	3.063
LR [24]	17.32
GNB [24]	0.347
DBAS-SLSTM [Proposed]	0.273

The comparative evaluation of various deep learning architectures for the task shows that traditional recurrent models like Bi-RNN, Bi-LSTM, and Bi-GRU achieved accuracies of 77.52%, 85.76%, and 83.52%, respectively. Adding attention mechanisms significantly improved performance, with Bi-LSTM + Attention reaching 92.88% and Bi-GRU + Attention achieving 94%. Advanced hybrid models such as Bi-CGRU + Attention attained 96.10%. The proposed DBAS-SLSTM outperformed all existing methods with the highest accuracy of 98.12%, demonstrating superior feature learning and classification capabilities. Table 6 shows the performance of models in the Motion Attitude Error Detection System.

Table 6: Accuracy comparison of motion error detection in physical exercise

Methods	Accuracy
Bi-LSTM [26]	85.76%
Bi-LSTM + Attention [26]	92.88%
RNN + Attention [26]	82%
Bi-RNN + Attention [26]	79.77%
Bi-RNN [26]	77.52%
Bi-CLSTM [26]	90.10%
Bi-CGRU + Attention [26]	96.10%
Bi-GRU [27]	83.52%
Bi-GRU + Attention [27]	94%
DBAS-SLSTM [Proposed]	98.12%

The comparison of human pose estimation methods shows that the proposed DBAS-SLSTM outperforms MSFF-CNN across all metrics. In particular, DBAS-SLSTM has a larger mAP of 83.4% than 78.6% of MSFF-CNN, which is more accurate in locating key points. It achieves a higher overall pose prediction, which is indicated by its PCK@0.5 score of 94.2%, which is higher than MSFF-CNN of 91.5%. DBAS-SLSTM has a higher key point accuracy of 91.3% compared to the 86.8% of MSFF-CNN, which further proves that it is better at estimating joints accurately. These measures were estimated through the process of extracting multi-sensor data streams, extracting joint key points, and comparing them with ground truth postures based on annotated reference movements. Additionally, DBAS-SLSTM offers faster inference at 31.5 FPS versus

27.3 FPS, making it both more accurate and efficient for real-time applications. Overall, DBAS-SLSTM is the superior method. Table 7 and Figure 15 display the system monitoring, evaluating, and correcting human movements efficiently.

Table 7: Real-time Multi-Sensor Motion Attitude Error Detection Visualization

Method	mAP(%)	Keypoint accuracy (%)	PCK@0.5 (%)	Inference speed (FPS)
MSFF-CNN [25]	78.6	86.8	91.5	27.3
DBAS-SLSTM [Proposed]	83.4	91.3	94.2	31.5

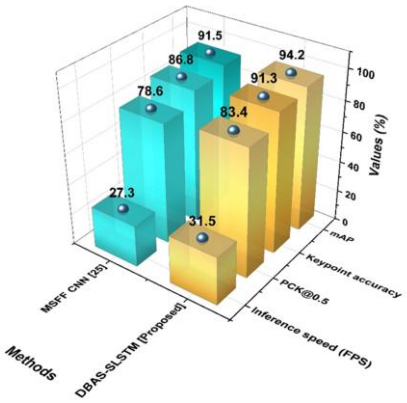

Figure 15: Performance Comparison of Pose Estimation Methods of mAP, keypoint accuracy, PCK@0.5, and Inference speed

4 Discussion and future work

The motion attitude error detection system utilizes multi-sensor data to continuously monitor and evaluate human movements, accurately identifying posture deviations in real time, enabling corrective feedback to enhance performance, prevent injuries, and optimize overall physical training outcomes. The existing methods had significant limitations. Conventional machine learning techniques like RF, DT, LR, and GNB [24] were fast and interpretable and cannot reflect complicated temporal correlations in high-dimensional motion data, thus cannot achieve a high level of accuracy. Deep learning models such as CNN and CNN-LSTM models [25] could be very sensitive to detect spatial features, although these models tend to fail to capture long-term temporal dynamics, making them less sensitive to minor deviations in posture. Bi-RNN, Bi-LSTM, Bi-CLSTM, and Bi-CGRU (with or without attention) [26,27] and bidirectional architectures enhance temporal modeling, but were characterized by high computational complexity and increased memory usage, longer inference time, and overfitting risks, limiting the practical implementation to real-time.

To overcome these limitations, the proposed DBAS-SLSTM network minimizes manual tuning and overfitting, and the proposed framework effectively learns both short-term and long-term temporal variations of multi-sensory data. As a result, the system attains enhanced accuracy, robustness, and real-time speed of motion attitude error detection in feasible healthcare applications.

Moreover, the system is developed in such a way that it has real-world flexibility. It is capable of accommodating variations in various users (body types and skill levels), exercise types, and moderate sensor noise or misalignments with multi-sensor fusion and adaptive DBAS parameter tuning. Initial analysis shows that there is a stable performance during these variations. Future efforts will concentrate on the widespread experimental research in the diverse real-life scenarios and improving resilience to extreme sensor errors to guarantee a dependable and exact feedback in the real-world application.

Although the proposed approach had shown good results in the analyzed and tested conditions, its extrapolability to unknown participants and activities has not been thoroughly tested. Differentiations in the morphology of the body and the manner of executing the exercises can influence the consistency of features, especially in high intra-class variation exercises. Future analyses will include cross-user and cross-exercise measures to measure robustness more accurately.

The future scope was integration with wearable devices, AI-driven personalized feedback, expanded movement libraries, and improved sensor fusion algorithms, which could enhance accuracy, adaptability, and real-time corrective guidance across rehabilitation, sports training, and ergonomics applications.

However, practical deployment may face challenges such as sensor calibration, maintaining data privacy, and ensuring participant safety, which should be carefully addressed during real-world implementation. The future application will introduce the system to portable embedded systems and wearable architecture to further lower the latency and test the real-time performance in field-based training set-ups to ensure useful utilization in the real-life exercise context.

5 Conclusion

A real-time Motion Attitude Error Detection System utilizes multi-sensor data to continuously monitor, evaluate, and correct human movements, enhancing performance accuracy, preventing injuries, and supporting safe, optimized physical training. The dataset was a Motion Attitude Error Detection System integrating various physical exercises. Through Kalman filtering, normalization, and wavelet-based feature extraction, the system captures detailed motion characteristics. The proposed DBAS-SLSTM framework effectively detects posture errors in real time and provides corrective feedback, demonstrating significant potential for enhancing exercise performance, injury prevention, and personalized training. The

proposed DBAS-SLSTM framework demonstrates high efficiency and performance, achieving a runtime of 0.273 s, accuracy of 98.12%, mAP of 83.4%, PCK@0.5 of 94.2%, and an inference speed of 31.5 FPS, indicating its capability for real-time, precise motion attitude error detection and corrective feedback. The system may face sensor noise, calibration errors, and limited adaptability to diverse body types or complex movements. Real-time processing can be computationally intensive, potentially affecting responsiveness.

Fund

This work was supported by the Young Talent Project of Hubei Provincial Department of Education Scientific Research Plan (Grant No. Q20244201) for the project titled "Real-time Police Action Recognition and Analysis System Based on Deep Learning Models" (Project Leader: Zhongyi Ni; Host Institution: Hubei University of Police).

Ethical considerations

Research presented in this study uses the Motion Attitude Error Detection Dataset obtained from Kaggle. The dataset was sourced as a publicly available resource intended for research and benchmarking in machine learning. Prior to its use, The dataset did not contain personally identifiable information (PII) or specific consent from individuals.

Informed consent

Research did not involve human participants or identifiable personal data; therefore, informed consent was not required. The dataset used is publicly available on Kaggle and was utilized strictly for research purposes in compliance with its usage terms.

References

[1] Vidya B, Sasikumar P. Wearable multi-sensor data fusion approach for human activity recognition using machine learning algorithms. Sensors and Actuators A: Physical, 2022, 341:113557. https://doi.org/10.1016/j.sna.2022.113557

[2] Huang C, Liu Y, Sun X, Wang Y. Intelligent active suspension control method based on hierarchical multi-sensor perception fusion. Sensors, 2025, 25(15):4723. https://doi.org/10.3390/s25154723

[3] Zhou L. Design of sports posture real-time monitoring system based on sensor data flow. Journal of Computational Methods in Science and Engineering, 2022, 22(6):2077–2091. https://doi.org/10.3233/JCM226400

[4] Lin FC, Ngo HH, Dow CR, Lam KH, Le HL. Student behavior recognition system for classroom environments based on skeleton pose estimation. Sensors, 2021, 21(16):5314. https://doi.org/10.3390/s21165314

[5] Liu C, Chang Z. Sensor and attitude analysis of track and field training action recognition based on artificial intelligence. Journal of Sensors, 2022, 2022:6282388. https://doi.org/10.1155/2022/6282388

[6] Xu Y. Real-Time Motion Recognition in Special Training Systems Based on the Optimized BBO-KNN Method of Motion Morphology. Informatica, 2025, 49(16). https://doi.org/10.31449/inf.v49i16.9600

[7] Chang R, Yang Z, Ning J. Inaccurate action detection algorithm for rowing machine exercise based on attention-CNN. IEEE Access, 2024, 12:114961–114973. https://doi.org/10.1109/ACCESS.2024.3445875

[8] Bu B. Evaluation on Numerical Method of Differential Formula Based on Optimal Control of Space Robot's Attitude and Motion. Informatica, 2024, 48(13). https://doi.org/10.31449/inf.v48i13.6065

[9] Lv Y, Li M, Li B. Athletic sports posture measurement algorithm based on multi-sensor combination. Journal of Computational Methods in Science and Engineering, 2022, 22(6):2065–2076. https://doi.org/10.3233/JCM-226393

[10] Wang J, Wang Z, Qiu S, Xu J, Zhao H, Fortino G, Habib M. A selection framework of sensor combination feature subset for human motion phase segmentation. Information Fusion, 2021, 70:1-11. https://doi.org/10.1016/j.inffus.2020.12.009

[11] Gu H, Jin C, Yuan H, Chen Y. Attitude and heading reference system using extended Kalman filter. International Journal of Uncertainty, Fuzziness and Knowledge-Based Systems, 2021, 29(Suppl.1):157–180. https://doi.org/10.1142/S0218488521400092

[12] Liu F, Liu Y, Sun X, Sang H. Hierarchical multi-sensor data fusion based on unscented Kalman filter. Applied Ocean Research, 2021, 109:102562. https://doi.org/10.1016/j.apor.2021.102562

[13] Li H. Motion trajectory monitoring system based on multi-sensor data fusion. Procedia Computer Science, 2025, 262:101–107. https://doi.org/10.1016/j.procs.2025.05.033

[14] Li J, Liu X, Wang Z, Zhao H, Zhang T, Qiu S, Cangelosi A. Real-time human motion capture based on wearable inertial sensor networks. IEEE Internet of Things Journal, 2021, 9(11):8953-8966. https://doi.org/10.1109/JIOT.2021.3119328

[15] Yang H, Wang Y, Wang H, Shi Y, Zhu L, Kuang Y, Yang Y. Multi-Inertial Sensor-Based Arm 3D Motion Tracking Using Elman Neural Network. Journal of Sensors, 2022, 2022(1):3926417. https://doi.org/10.1155/2022/3926417

[16] Liu Q. Human motion state recognition based on MEMS sensors and Zigbee network. Computer Communications, 2022, 181:164–172. https://doi.org/10.1016/j.comcom.2021.10.018

[17] Brunson B, Wang J, Ma W. Modeling of IMU arrays under generic multi-sensor integration strategy. Sensors, 2024, 24(23):7754. https://doi.org/10.3390/s24237754

[18] Zhong Y, Chen X, Gao N, Jiao Z. In-motion alignment with MEMS-IMU using multilocal linearization detection. Sensors, 2025, 25(9):2645. https://doi.org/10.3390/s25092645

[19] Hajjej F, Javeed M, Ksibi A, Alarfaj M, Alnowaiser K, Jalal A, Park J. Deep human motion detection and multi-features analysis for smart healthcare learning tools. Ieee Access, 2022, 10: 116527-116539. https://doi.org/10.1109/ACCESS.2022.3214986

[20] Dai A, Xiao Y, Shen H, Zhi S, Long D. Anomaly detection of spacecraft inertial measurement units using multi-scale dependency neural network. Acta Astronautica, 2025, 232:204–214. https://doi.org/10.1016/j.actaastro.2025.03.014

[21] Li J, Liu X, Wang Z, Zhang T, Qiu S, Zhao H, Cangelosi A. Real-time hand gesture tracking for human–computer interface based on multi-sensor data fusion. IEEE Sensors Journal, 2021, 21(23):26642-26654. https://doi.org/10.1109/JSEN.2021.3122236

[22] Gu Y, Han Y, Liu X, Zhang N, Zhang X, Pan M, Liu, T. A flexible sensor and mimu-based multisensor wearable system for human motion analysis. IEEE Sensors Journal, 2023, 23(4):4107-4117. https://doi.org/10.1109/JSEN.2022.3233653

[23] Liu W, Liu Y, Bucknall R. Filtering-based multi-sensor data fusion for unmanned surface vehicle navigation. Journal of Marine Engineering & Technology, 2023, 22(2):67–83. https://doi.org/10.1080/20464177.2022.2031558

[24] Naseer A, Raza A, Afzal H, Smerat A, Fitriyani NL, Gu Y, Syafrudin M. Human pose estimation in physiotherapy fitness exercise correction using novel transfer learning approach. PeerJ Computer Science, 2025, 11:e2854.

[25] Chen H, Fan R. Improved convolutional neural network for precise exercise posture recognition and health indicator prediction. Scientific Reports, 2025, 15(1):21309. https://doi.org/10.1038/s41598-025-01854-x

[26] Rao P, Asha CS, Rao PR. Real-time posture correction of squat exercise using deep learning. IEEE Access, 2025, 13:39557–39571. https://doi.org/10.1109/ACCESS.2025.3545207

[27] Chariar M, Rao S, Irani A, Suresh S, Asha CS. AI trainer: Autoencoder based approach for squat analysis and correction. IEEE Access, 2023, 11:107135-107149. https://doi.org/10.1109/ACCESS.2023.3316009